



Effect of Height Variation on Coefficient of Discharge for Crump Weir

Sani Yakubu Khalifa

Department of Water Resources and Environmental Engineering,
Ahmadu Bello University Zaria, Kaduna state, Nigeria.

ABSTRACT

A crump weir is commonly used to measure discharge in open flow channels. The objective of this study was to determine the effect of surface roughness of crump weir. 18 crump weir models of different apex angle 80° , 90° , 100° , 110° , 120° and 130° . Also by decreasing upstream angles to have the following values 85° , 70° , 55° , 40° , 25° and 10° . The increasing values of the downstream angles are 15° , 20° , 25° , 30° , 35° and 40° respectively to obtain the sum angle of the triangle to be 180° were developed. For each type of crump three types of surface roughness were used. The first one was a smooth PVC, the second one is coated with a uniform sand $D_{50}=1.18\text{mm}$ (D_{50} is the sieve diameter in which 50% of material are finer), while the third is covered by gravel of $D_{50}=4.0\text{mm}$. Eighteen models were used to conduct an experimental study. From the result obtained model 17 is the most efficient crump weir having the least C_d of 1.14914 and least percentage error of 12.97412. And the model has been optimized using GA with C_d value of 1.14815. The obtained results show that C_d values increase with increasing flow rate as well as with decreasing crump height; an increase in surface roughness of crump weir can make a great reduction in C_d value. The h/P effect on C_d values increases with an increase in crump weir height. The C_d value is also directly proportional to the upstream slope and inversely to the downstream slope.

ARTICLE INFO

Article History

Received: August, 2020

Received in revised form: October, 2020

Accepted: January, 2021

Published online: January, 2021

KEYWORDS

Crump Weir, Discharge Coefficient, Energy Dissipation, Hydraulic Jump, Hydraulic Structure, Open Channels

INTRODUCTION

The Crump section flat-vee weir is favored by hydrometrics' because of the accuracy and range of flow measurement, but is disliked by fisheries officers because it can present a barrier to fish migration. [Rickard *et.al.*2003]. It is very important to investigate the behavior of the flow over the crump weir. A few number of studies have been devoted to the flow over this type of weirs, [Bos, 1989] was the first to study the flow characteristics of trapezoidal profile weirs systematically. He conducted a series of experiments on these types of weirs with both upstream and downstream side slopes.

The discharge coefficient was determined for free flow conditions using different discharge values. (Al-Naely *et al.*, 2018) Hydraulic Structures such as crump weir are placed in channels to estimate or measure flow rate and flow control devices. In this study there is a new performance for crump weir which appears by adding opening holes in the model of crump weir. Opening holes are working as an energy dissipater and as an improver for the discharge coefficient (C_d). Where the discharge coefficient (C_d) is improved and recorded a higher values in comparison with conventional weir under the same laboratory conditions. (Khalifa &

Umar, 2018) A crump weir is commonly used to measure discharge in open flow channels. The laboratory test was conducted on six crump weir models of different apex angles 80°, 90° 100°, 110° 120° and 130°.

Increasing the amount of flow rate in different structures was always a field of interest for researchers. Decreasing sedimentation in reservoirs (Zahabi et al. 2018) and the creation of an opening in a broad-crested weir body to increase the discharge coefficient (Daneshfaraz et al. 2019) are examples of improving the flow rate. The other vital structures that can control the flow rate are weirs. The volume of flow over the weirs depends on the length and shape of the crest of the weir. Many types of research have been done on the effect of the hydraulic and geometric parameters on the C_d and the amount of flow discharged effective ways to increase the weir length at a given width is to use weirs with nonlinear plans such as triangular, trapezoidal, circular, and parabolic.

Crump weir has many features such as straightforward structure, giving high precision in flow measurement. Also, it is comparatively insensitive to submerged conditions and ease of determination of flow curves for any width. In addition to that, it has many advantages like the coefficient of

discharges remains stable and constants through undrown condition; and moderately unresponsive to drowned condition.

THEORETICAL BACKGROUND

The discharge equation for the crump weir was used to compute the estimated discharge using the flow heads. Point gauge will be used to measure the flow head (h) above the crump weir (Arora, 2005).

$$Q_m = C_d \sqrt{g} \cdot b H_o^{\frac{3}{2}} \quad (1)$$

$$C_d = 1.163 \left(1 - \frac{0.0003}{h} \right)^{1.5} \quad (2)$$

$$H = y + \frac{v^2}{2g} \quad (3)$$

$$f = Q/Q_m, \quad (4)$$

METHODOLOGY

Fabrication of the Experimental Models

The experimental work was conducted on six crump weir models of different apex angles 80°, 90° 100°, 110° 120° and 130°. Also by decreasing upstream angles to have the following values 85°, 70°, 55°, 40°, 25° and 10°. The increasing values of the downstream angles are 15°, 20°, 25°, 30°, 35° and 40° respectively to obtain the sum angle of the triangle to be 180°. Plywood of thickness 22mm was used for fabricating the main body of the crump weir.

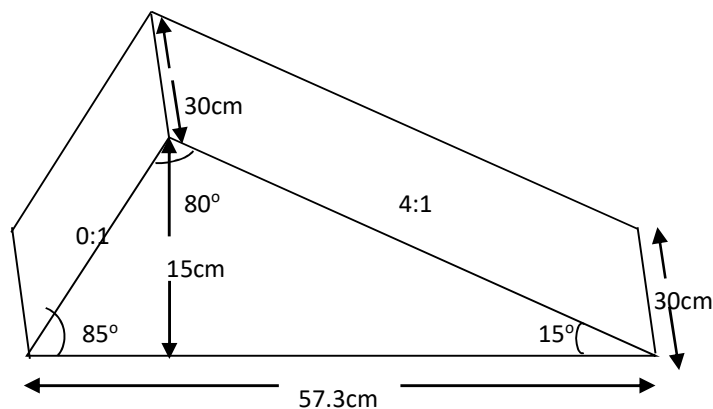


Figure 1: The schematic view of crump weir model 1 of apex angle 80°, upstream angle and slope, 85° and 0:1, downstream angle and slope, 15° and 4:1 respectively.

Corresponding author: Yakubu, S. K. ✉ Khalees2k1@gmail.com, ✉ Department of Water Resources and Environmental Engineering, A. B. U., Zaria. © 2021 Faculty of Tech. Education, ATBU Bauchi. All rights reserved

Table 1.0: Geometric Factors of Crump Weir Models

| Model | Upstream Slope | Downstream Slope | Model width 'b' (cm) | Crest Height 'P' (cm) | Apex Angle (degree) | Upstream Angle(degree) | Downstream Angle(degree) |
|-------|----------------|------------------|----------------------|-----------------------|---------------------|------------------------|--------------------------|
| 7 | 0:1 | 4:1 | 30 | 15 | 80 | 85 | 15 |
| 8 | 0:3 | 3:1 | 30 | 15 | 90 | 70 | 20 |
| 9 | 0:7 | 2:1 | 30 | 15 | 100 | 55 | 25 |
| 10 | 1:1 | 2:1 | 30 | 15 | 110 | 40 | 30 |
| 11 | 2:1 | 1:1 | 30 | 15 | 120 | 25 | 35 |
| 12 | 6:1 | 1:1 | 30 | 15 | 130 | 10 | 40 |



Plate I: Side view of the Tilting Flume



Plate VII: Model 6 of apex angle 130° , upstream angle and slope, 10° and 6:1, downstream angle and slope, 40° and 1:1 respectively.

Experimental Procedure

The crump weir were installed in the flume with the help of sealants to prevent leakage, which has to be levelled. One vernier were located downstream the weir and the other upstream. The verniers were zeroed with the bed of the channel.

Fifty-Four models were fabricated for which the angles were varied, 80° , 90° , 100° , 110° , 120° , and 130°

Experiment were then be ran for each model and various heads and their corresponding discharges were recorded; the procedure has five (5) runs. Each run has a different flow rate and a set of four (4) y_0 and y_1 depths; two sets for modular flow

Corresponding author: Yakubu, S. K. ✉ Khalees2k1@gmail.com, ✉ Department of Water Resources and Environmental Engineering, A. B. U., Zaria. © 2021 Faculty of Tech. Education, ATBU Bauchi. All rights reserved



condition and the other two sets for non-modular flow condition. The initial flow rate was set. Then, y_0 and y_1 depths were recorded for the following conditions: Modular flow: without stop block (gate). Modular flow: one full stop block (gate) (y_1 should be the only depth that changes). Non-modular flow: Add half of the one-stop block (gate). (y_1 and y_0 depth that change). Non-modular flow: Add one-quarter of a stop block (gate). The flow rate was increased at a constant interval.

Heights (P=10cm, 15cm, 20cm) were used as a crump weir models. For each type of crump three types of surface roughness were used. The first one was a smooth PVC, the second one is coated with a uniform sand $D_{50}=0.72\text{mm}$ (D_{50} is the sieve diameter in which 50% of material are finer), while the third is covered by gravel of $D_{50}=3.6\text{ mm}$. Eighteen models were used to conduct an experimental study. In each run, the selected model was inserted along the width of the flume. Then the pump started at the desired flow rate and after the flow stability was achieved the water surface level upstream and above the weir model were measured using a point gauge. For each type of crump weir, a series of tests under different flow rates were conducted. The pump was activated and the discharge was adjusted using a control valve and the reading of the point gauge were recorded to give the head above the crump weir required for the calculation of estimated discharge; At the beginning of each run the control valve was adjusted to alter the head; For each head recorded, the actual discharge was measured by the direct method using the weighing arrangement provided at the tail end of the flume; The previous steps were repeated for each of the five runs of experiments to be conducted for each model. A total of 360 runs were conducted.

Determination of Observed Discharge (Q_o)

The observed discharge, Q_o , was measured experimentally using the gravimetric method. Throughout the experiment, 100kg of water were collected using the weighing balance (see plate II) attached to the flume and a stopwatch was used to obtain the time taken to collect the 100kg for onward determination of discharge.

Volume, $V = \text{mass}/\text{density}$

Observed discharge, $Q_o = \text{Volume} / \text{average time}$

$$\text{Average time} = \frac{(t_1 + t_2)}{2} \quad (5)$$

Determination of Estimated Discharge (Q_e)

The discharge equation for the crump weir was used to compute the estimated discharge using the flow heads. Point gauge will be used to measure the flow head (h) above the crump weir (Arora, 2005).

$$Q_m = C_d \sqrt{g} \cdot b H_o^{\frac{3}{2}} \quad (1)$$

$$C_d = 1.163 \left(1 - \frac{0.0003}{h} \right)^{1.5} \quad (2)$$

$$H = y + \frac{v^2}{2g} \quad (3)$$

Accuracy of Discharge Measurement

In this study, the indicator employed to compare the accuracy of the crump weir models in measuring discharge is the average percentage error (E) expressed as:

$$E = \frac{100}{N} \sum_{i=1}^N \left| \frac{Q_o - Q_e}{Q_o} \right| \quad (6)$$

Where N = number of experiments conducted per model

Q_o And Q_e are observed and estimated discharges obtained for each run.

Derivation of Discharge Coefficient

The discharge coefficients for simple rectangular and triangular weirs suggested respectively by French (1986) and Martinez et al. (2005) were adopted in this study. The expression for the global discharge coefficient (C_d) of the models was



obtained by multiple regressions of the variables (i.e. h/P , C_d , and b).

To validate the suitability of the theoretical equations, the maximum of the absolute value of the deviation of the data from the model was obtained as:

$$\text{MaxErr} = \max(\text{abs}(C_{do} - C_{de})) \quad (7)$$

Where, C_{do} = Experimental Discharge Coefficient = Q_o / Q_e

C_{de} = Estimated Discharge Coefficient

$$Cd = (D_{50}, P, h, Q, \theta) \quad (8)$$

Thus, by dimensional analysis and using the approach of Buckingham's π -theorem, Equation (8) becomes:

$$Cd = f\left(\frac{D_{50}}{P}, \theta, \frac{h}{P}\right) \quad (9)$$

It follows that Equation (9) can be expressed as Equation (10) based on dimensional homogeneity:

$$C_d = k_1 \left[\frac{D_{50}\theta}{P}\right]^a + k_2 \left[\frac{h}{P}\right]^b \quad (10)$$

Where, K_1 , K_2 , a , and b are parameters to be estimated by regression analysis.

RESULTS AND DISCUSSION

Computation of Discharge Coefficients (C_d)

Tables 2 show the values of C_d obtained from Equations 1 and 2 respectively. The head measurements were obtained using the point gauge.

Table 2: Discharge characteristics for model 1:

| $Q_o=V/t/m^3/s$ | y_o/m | $h_o=y_o - 0.10/m$ | y_1/m | H_o/m | H_1/m | C_d | $Q_e/m^3/s$ | % Error |
|-----------------|---------|--------------------|---------|---------|---------|---------|-------------|----------|
| 0.001515 | 0.120 | 0.020 | 0.060 | 0.121 | 0.065 | 1.13693 | 0.00133 | 12.04391 |
| 0.001563 | 0.160 | 0.060 | 0.110 | 0.175 | 0.115 | 1.15429 | 0.00135 | 13.36654 |
| 0.001613 | 0.194 | 0.094 | 0.135 | 0.210 | 0.140 | 1.15744 | 0.00139 | 13.60220 |
| 0.001667 | 0.210 | 0.110 | 0.130 | 0.228 | 0.150 | 1.15825 | 0.00144 | 13.66252 |
| 0.001724 | 0.218 | 0.118 | 0.100 | 0.235 | 0.160 | 1.15857 | 0.00149 | 13.68652 |
| Average | | | | | | 1.15310 | 0.001400 | 13.27234 |

ii. Estimated discharge and C_d for PVC

| $Q_o=V/t/m^3/s$ | y_o/m | $h_o=y_o - 0.10/m$ | y_1/m | H_o/m | H_1/m | C_d | $Q_e/m^3/s$ | % Error |
|-----------------|---------|--------------------|---------|---------|---------|---------|-------------|----------|
| 0.00150 | 0.125 | 0.025 | 0.060 | 0.130 | 0.060 | 1.14213 | 0.00131 | 12.44421 |
| 0.00158 | 0.167 | 0.067 | 0.100 | 0.177 | 0.110 | 1.15520 | 0.00136 | 13.43472 |
| 0.00164 | 0.193 | 0.093 | 0.120 | 0.208 | 0.140 | 1.15738 | 0.00142 | 13.59774 |
| 0.00170 | 0.208 | 0.108 | 0.060 | 0.227 | 0.150 | 1.15816 | 0.00146 | 13.65596 |
| 0.00175 | 0.215 | 0.115 | 0.060 | 0.232 | 0.150 | 1.15845 | 0.00151 | 13.67792 |
| Average | | | | | | 1.15426 | 0.001412 | 13.36211 |

iii. Estimated discharge and C_d for 1.18mm

| $Q_o=V/t/m^3/s$ | y_o/m | $h_o=y_o - 0.10/m$ | y_1/m | H_o/m | H_1/m | C_d | $Q_e/m^3/s$ | % Error |
|-----------------|---------|--------------------|---------|---------|---------|---------|-------------|----------|
| 0.001579 | 0.127 | 0.027 | 0.060 | 0.130 | 0.060 | 1.14367 | 0.00138 | 12.56224 |
| 0.001639 | 0.170 | 0.070 | 0.100 | 0.180 | 0.100 | 1.15553 | 0.00142 | 13.45974 |
| 0.006969 | 0.195 | 0.095 | 0.135 | 0.210 | 0.135 | 1.15750 | 0.00602 | 13.60657 |
| 0.001695 | 0.210 | 0.110 | 0.060 | 0.225 | 0.060 | 1.15825 | 0.00146 | 13.66252 |
| 0.001818 | 0.218 | 0.118 | 0.070 | 0.235 | 0.070 | 1.15857 | 0.00157 | 13.68652 |
| Average | | | | | | 1.15470 | 0.002370 | 13.39552 |

Corresponding author: Yakubu, S. K. ✉ Khalees2k1@gmail.com, ✉ Department of Water Resources and Environmental Engineering, A. B. U., Zaria. © 2021 Faculty of Tech. Education, ATBU Bauchi. All rights reserved



iv Estimated discharge and C_d for 4.00mm

| $Q_0=V/t/m^3/s$ | y_0/m | $h_0=y_0 - 0.10/m$ | y_1/m | H_0/m | H_1/m | C_d | $Q_e/m^3/s$ | % Error |
|-----------------|---------|--------------------|---------|---------|---------|---------|-------------|----------|
| 0.001456 | 0.128 | 0.028 | 0.060 | 0.130 | 0.060 | 1.14436 | 0.00127 | 12.61484 |
| 0.001563 | 0.171 | 0.071 | 0.105 | 0.180 | 0.105 | 1.15564 | 0.00135 | 13.46761 |
| 0.001613 | 0.198 | 0.098 | 0.135 | 0.213 | 0.135 | 1.15766 | 0.00139 | 13.61913 |
| 0.001667 | 0.212 | 0.112 | 0.060 | 0.230 | 0.060 | 1.15833 | 0.00144 | 13.66884 |
| 0.001754 | 0.220 | 0.120 | 0.070 | 0.238 | 0.070 | 1.15864 | 0.00151 | 13.69202 |
| Average | | | | | | 1.15493 | 0.001392 | 13.41249 |

Table 4.3: Summary of models performance

| Model 1 | θ_A | θ_u | θ_d | Range of Q_0 (l/s) | Range of Q_e (l/s) | Average C_d | E (%) | Rank |
|----------------------------|-------------|------------|------------|----------------------|----------------------|---------------|----------|------|
| N | 80° | 85° | 15° | 6.781 – 8.228 | 5.881 – 7.128 | 1.15310 | 13.27234 | 9 |
| PVC | 80° | 85° | 15° | 6.781 – 8.228 | 5.881 – 7.128 | 1.15426 | 13.36211 | |
| 1.8mm | 80° | 85° | 15° | 6.781 – 8.228 | 5.879 – 7.123 | 1.15470 | 13.39552 | |
| 4.0mm | 80° | 85° | 15° | 6.781 – 8.228 | 5.877 – 7.121 | 1.15493 | 13.41249 | |
| Average $C_d = 1.15425$ | | | | | | 13.36062 | | |
| Model 2 | | | | | | | | |
| N | 90° | 70° | 20° | 4.644 – 7.813 | 4.033 – 6.775 | 0.98353 | 1.68016 | 2 |
| PVC | 90° | 70° | 20° | 4.644 – 7.813 | 4.033 – 6.775 | 0.97408 | 2.70565 | |
| 1.8mm | 90° | 70° | 20° | 4.644 – 7.813 | 4.032 – 6.770 | 0.98483 | 1.54263 | |
| 4.0mm | 90° | 70° | 20° | 4.644 – 7.813 | 4.032 – 6.769 | 0.98511 | 1.54263 | |
| Average $C_{d0} = 0.98189$ | | | | | | 1.86777 | | |
| Model 3 | | | | | | | | |
| N | 100° | 55° | 25° | 4.601 – 6.110 | 4.000 – 5.301 | 1.15412 | 13.35118 | 13 |
| PVC | 100° | 55° | 25° | 4.601 – 6.110 | 4.000 – 5.301 | 1.15422 | 13.35942 | |
| 1.8mm | 100° | 55° | 25° | 4.601 – 6.110 | 3.997 – 5.300 | 1.15456 | 13.38700 | |
| 4.0mm | 100° | 55° | 25° | 4.601 – 6.110 | 3.996 – 5.299 | 1.15507 | 13.42232 | |
| Average $C_{d0} = 1.15449$ | | | | | | 13.37998 | | |

The ranking is based on the closeness of average C_d to unity and also on the minimum average percentage error (E)

| Model 7 | θ_A | θ_u | θ_d | Range of Q_0 (l/s) | Range of Q_e (l/s) | Average C_d | E (%) | Rank |
|-------------------------|------------|------------|------------|----------------------|----------------------|---------------|----------|------|
| N | 80° | 85° | 15° | 6.781 – 8.228 | 5.881 – 7.128 | 1.15324 | 13.28325 | 8 |
| PVC | 80° | 85° | 15° | 6.781 – 8.228 | 5.881 – 7.128 | 1.15382 | 13.32825 | |
| 1.8mm | 80° | 85° | 15° | 6.781 – 8.228 | 5.879 – 7.123 | 1.15450 | 13.37952 | |
| 4.0mm | 80° | 85° | 5° | 6.781 – 8.228 | 5.877 – 7.121 | 1.15501 | 13.41841 | |
| Average $C_d = 1.15414$ | | | | | | 13.35236 | | |
| Model 8 | | | | | | | | |
| N | 90° | 70° | 20° | 4.644 – 7.813 | 4.033 – 6.775 | 0.97358 | 2.72040 | |



| Model | θ_A | θ_u | θ_d | Range of Q_o (l/s) | Range of Q_e (l/s) | Average C_{do} | E (%) | Rank |
|----------------------------|------------------|-----------------|-----------------|-------------------------|-------------------------|---------------------|----------|------|
| Model 4 | | | | | | | | |
| N | 110 ⁰ | 40 ⁰ | 30 ⁰ | 5.000 – 5.941 | 4.348 – 5.154 | 0.95249 | 4.99514 | 5 |
| PVC | 110 ⁰ | 40 ⁰ | 30 ⁰ | 5.000 – 5.941 | 4.348 – 5.154 | 0.95316 | 4.91923 | |
| 1.8mm | 110 ⁰ | 40 ⁰ | 30 ⁰ | 5.000 – 5.941 | 4.346 – 5.153 | 0.95305 | 4.93159 | |
| 4.0mm | 110 ⁰ | 40 ⁰ | 30 ⁰ | 5.000 – 5.941 | 4.345 – 5.152 | 0.95381 | 4.84463 | |
| Average C_{do} = 0.95313 | | | | | | 4.92315 | | |
| Model 5 | | | | | | | | |
| N | 120 ⁰ | 25 ⁰ | 35 ⁰ | 4.967 – 6.098 | 4.322 – 5.292 | 1.15339 | 13.29607 | 7 |
| PVC | 120 ⁰ | 25 ⁰ | 35 ⁰ | 4.967 – 6.098 | 4.322 – 5.292 | 1.15382 | 13.32874 | |
| 1.8mm | 120 ⁰ | 25 ⁰ | 35 ⁰ | 4.967 – 6.098 | 4.321 – 5.291 | 1.15411 | 13.35135 | |
| 4.0mm | 120 ⁰ | 25 ⁰ | 35 ⁰ | 4.967 – 6.098 | 4.319 – 5.291 | 1.15493 | 13.41346 | |
| Average C_{do} = 1.15406 | | | | | | 13.34741 | | |
| Model 6 | | | | | | | | |
| N | 130 ⁰ | 10 ⁰ | 40 ⁰ | 4.800 – 6.263 | 4.178 – 5.440 | 1.15419 | 13.35648 | 18 |
| PVC | 130 ⁰ | 10 ⁰ | 40 ⁰ | 4.800 – 6.263 | 4.178 – 5.440 | 1.15514 | 13.42857 | |
| 1.8mm | 130 ⁰ | 10 ⁰ | 40 ⁰ | 4.800 – 6.263 | 4.177 – 5.438 | 1.15631 | 13.51699 | |
| 4.0mm | 130 ⁰ | 10 ⁰ | 40 ⁰ | 4.800 – 6.263 | 4.175 – 5.437 | 1.15647 | 13.52889 | |
| Average C_{do} = 1.15553 | | | | | | 13.45773 | | |
| PVC | 90 ⁰ | 70 ⁰ | 20 ⁰ | 4.644 – 7.813 | 4.033 – 6.775 | 0.97537 | 2.52810 | 3 |
| 1.8mm | 90 ⁰ | 70 ⁰ | 20 ⁰ | 4.644 – 7.813 | 4.032 – 6.770 | 0.97580 | 2.48215 | |
| 4.0mm | 90 ⁰ | 70 ⁰ | 20 ⁰ | 4.644 – 7.813 | 4.032 – 6.769 | 0.97612 | 2.44822 | |
| Average C_{do} = 0.97522 | | | | | | 2.54472 | | |
| Model 9 | | | | | | | | |
| N | 100 ⁰ | 55 ⁰ | 25 ⁰ | 4.601 – 6.110 | 4.000 – 5.301 | 1.15374 | 13.32206 | 15 |
| PVC | 100 ⁰ | 55 ⁰ | 25 ⁰ | 4.601 – 6.110 | 4.000 – 5.301 | 1.15486 | 13.40714 | |
| 1.8mm | 100 ⁰ | 55 ⁰ | 25 ⁰ | 4.601 – 6.110 | 3.997 – 5.300 | 1.15520 | 13.43317 | |
| 4.0mm | 100 ⁰ | 55 ⁰ | 25 ⁰ | 4.601 – 6.110 | 3.996 – 5.299 | 1.15550 | 13.45584 | |
| Average C_{do} = 1.15483 | | | | | | 13.40455 | | |
| Model 10 | | | | | | | | |
| N | 80 ⁰ | 85 ⁰ | 15 ⁰ | 6.781 – 8.228 | 5.881 – 7.128 | 1.15377 | 13.32509 | 11 |
| PVC | 80 ⁰ | 85 ⁰ | 15 ⁰ | 6.781 – 8.228 | 5.881 – 7.128 | 1.15415 | 13.35366 | |
| 1.8mm | 80 ⁰ | 85 ⁰ | 15 ⁰ | 6.781 – 8.228 | 5.879 – 7.123 | 1.15443 | 13.37462 | |
| 4.0mm | 80 ⁰ | 85 ⁰ | 5 ⁰ | 6.781 – 8.228 | 5.877 – 7.121 | 1.15496 | 13.41562 | |
| Average C_d = 1.15433 | | | | | | 13.36725 | | |
| Model 11 | | | | | | | | |
| N | 90 ⁰ | 70 ⁰ | 20 ⁰ | 4.644 – 7.813 | 4.033 – 6.775 | 1.15381 | 13.32835 | 10 |
| PVC | 90 ⁰ | 70 ⁰ | 20 ⁰ | 4.644 – 7.813 | 4.033 – 6.775 | 1.15391 | 13.33570 | |
| 1.8mm | 90 ⁰ | 70 ⁰ | 20 ⁰ | 4.644 – 7.813 | 4.032 – 6.770 | 1.15436 | 13.37018 | |
| 4.0mm | 90 ⁰ | 70 ⁰ | 20 ⁰ | 4.644 – 7.813 | 4.032 – 6.769 | 1.15491 | 13.41198 | |
| Average C_{do} = 1.15425 | | | | | | 13.36155 | | |



| Model 12 | | | | | | | | |
|---------------------------|------------------|-----------------|-----------------|---------------|---------------|---------|----------|----|
| N | 100 ⁰ | 55 ⁰ | 25 ⁰ | 4.601 – 6.110 | 4.000 – 5.301 | 1.15430 | 13.36441 | 16 |
| PVC | 100 ⁰ | 55 ⁰ | 25 ⁰ | 4.601 – 6.110 | 4.000 – 5.301 | 1.15534 | 13.44349 | |
| 1.8mm | 100 ⁰ | 55 ⁰ | 25 ⁰ | 4.601 – 6.110 | 3.997 – 5.300 | 1.15544 | 13.45085 | |
| 4.0mm | 100 ⁰ | 55 ⁰ | 25 ⁰ | 4.601 – 6.110 | 3.996 – 5.299 | 1.15599 | 13.49322 | |
| Average C _{do} = | | | | | | 1.15527 | 13.43799 | |

| Model 13 | θ_A | θ_u | θ_d | Range of Q _o (l/s) | Range of Q _e (l/s) | Average C _d | E (%) | Rank |
|--------------------------|-----------------|-----------------|-----------------|----------------------------------|----------------------------------|------------------------|----------|------|
| N | 80 ⁰ | 85 ⁰ | 15 ⁰ | 6.781 – 8.228 | 5.881 – 7.128 | 1.15167 | 13.16045 | 12 |
| PVC | 80 ⁰ | 85 ⁰ | 15 ⁰ | 6.781 – 8.228 | 5.881 – 7.128 | 1.15404 | 13.34454 | |
| 1.8mm | 80 ⁰ | 85 ⁰ | 15 ⁰ | 6.781 – 8.228 | 5.879 – 7.123 | 1.15583 | 13.48113 | |
| 4.0mm | 80 ⁰ | 85 ⁰ | 5 ⁰ | 6.781 – 8.228 | 5.877 – 7.121 | 1.15605 | 13.49777 | |
| Average C _d = | | | | | | 1.15440 | 13.37097 | |

| Model 14 | | | | | | | | |
|---------------------------|-----------------|-----------------|-----------------|---------------|---------------|---------|----------|----|
| N | 90 ⁰ | 70 ⁰ | 20 ⁰ | 4.644 – 7.813 | 4.033 – 6.775 | 1.15364 | 13.31350 | 14 |
| PVC | 90 ⁰ | 70 ⁰ | 20 ⁰ | 4.644 – 7.813 | 4.033 – 6.775 | 1.15453 | 13.38235 | |
| 1.8mm | 90 ⁰ | 70 ⁰ | 20 ⁰ | 4.644 – 7.813 | 4.032 – 6.770 | 1.15509 | 13.42494 | |
| 4.0mm | 90 ⁰ | 70 ⁰ | 20 ⁰ | 4.644 – 7.813 | 4.032 – 6.769 | 1.15579 | 13.47772 | |
| Average C _{do} = | | | | | | 1.15476 | 13.39963 | |

| Model 15 | | | | | | | | |
|---------------------------|------------------|-----------------|-----------------|---------------|---------------|---------|----------|---|
| N | 100 ⁰ | 55 ⁰ | 25 ⁰ | 4.601 – 6.110 | 4.000 – 5.301 | 1.15301 | 13.26625 | 6 |
| PVC | 100 ⁰ | 55 ⁰ | 25 ⁰ | 4.601 – 6.110 | 4.000 – 5.301 | 1.15416 | 13.35474 | |
| 1.8mm | 100 ⁰ | 55 ⁰ | 25 ⁰ | 4.601 – 6.110 | 3.997 – 5.300 | 1.15376 | 13.32339 | |
| 4.0mm | 100 ⁰ | 55 ⁰ | 25 ⁰ | 4.601 – 6.110 | 3.996 – 5.299 | 1.15438 | 13.37060 | |
| Average C _{do} = | | | | | | 1.15383 | 13.32875 | |

| Model 16 | θ_A | θ_u | θ_d | Range of Q _o (l/s) | Range of Q _e (l/s) | Average C _d | E (%) | Rank |
|--------------------------|-----------------|-----------------|-----------------|----------------------------------|----------------------------------|------------------------|---------|------|
| N | 80 ⁰ | 85 ⁰ | 15 ⁰ | 6.781 – 8.228 | 5.881 – 7.128 | 0.96112 | 4.06018 | 4 |
| PVC | 80 ⁰ | 85 ⁰ | 15 ⁰ | 6.781 – 8.228 | 5.881 – 7.128 | 0.96112 | 4.06018 | |
| 1.8mm | 80 ⁰ | 85 ⁰ | 15 ⁰ | 6.781 – 8.228 | 5.879 – 7.123 | 0.96303 | 3.84641 | |
| 4.0mm | 80 ⁰ | 85 ⁰ | 15 ⁰ | 6.781 – 8.228 | 5.877 – 7.121 | 0.96364 | 3.77912 | |
| Average C _d = | | | | | | 0.96223 | 3.93647 | |

| Model 17 | | | | | | | | |
|---------------------------|-----------------|-----------------|-----------------|---------------|---------------|---------|---------|---|
| N | 90 ⁰ | 70 ⁰ | 20 ⁰ | 4.644 – 7.813 | 4.033 – 6.775 | 0.99093 | 0.92858 | 1 |
| PVC | 90 ⁰ | 70 ⁰ | 20 ⁰ | 4.644 – 7.813 | 4.033 – 6.775 | 0.98596 | 1.42666 | |
| 1.8mm | 90 ⁰ | 70 ⁰ | 20 ⁰ | 4.644 – 7.813 | 4.032 – 6.770 | 0.98895 | 1.12130 | |
| 4.0mm | 90 ⁰ | 70 ⁰ | 20 ⁰ | 4.644 – 7.813 | 4.032 – 6.769 | 0.98872 | 1.14571 | |
| Average C _{do} = | | | | | | 0.98864 | 1.15556 | |

| Model 18 | | | | | | | | |
|----------|------------------|-----------------|-----------------|---------------|---------------|---------|----------|--|
| N | 100 ⁰ | 55 ⁰ | 25 ⁰ | 4.601 – 6.110 | 4.000 – 5.301 | 1.15506 | 13.42245 | |



| | | | | | | | | |
|-----------------------------------|------------------|-----------------|-----------------|---------------|---------------|---------|----------|----|
| PVC | 100 ⁰ | 55 ⁰ | 25 ⁰ | 4.601 – 6.110 | 4.000 – 5.301 | 1.15532 | 13.44080 | 17 |
| 1.8mm | 100 ⁰ | 55 ⁰ | 25 ⁰ | 4.601 – 6.110 | 3.997 – 5.300 | 1.15540 | 13.44853 | |
| 4.0mm | 100 ⁰ | 55 ⁰ | 25 ⁰ | 4.601 – 6.110 | 3.996 – 5.299 | 1.15605 | 13.49741 | |
| Average C _{d0} = 1.15546 | | | | | | | 13.45230 | |

Table 4.4: Summary of models performance based on the dependence of Q₀ on h₀

| Model | R ² | % | Ranking |
|-------|----------------|------|---------|
| 4 | 0.831 | 83.1 | 5 |
| 16 | 0.870 | 87.0 | 4 |
| 15 | 0.674 | 67.4 | 6 |
| 8 | 0.873 | 87.3 | 3 |
| 2 | 0.879 | 87.9 | 2 |
| 17 | 0.984 | 98.4 | 1 |

The ranking is based on the strong dependence of discharge on the upstream water head above the crest

Table 3: Summary of models performance based on Cd and Percentage Error

| Model Number | Cd Average | Percentage Error | Ranking |
|--------------|------------|------------------|---------|
| 17 | 1.14914 | 12.97412 | 1 |
| 2 | 1.15189 | 13.17617 | 2 |
| 8 | 1.15122 | 13.18413 | 3 |
| 16 | 1.15223 | 13.20521 | 4 |
| 4 | 1.15313 | 13.27629 | 5 |
| 15 | 1.15383 | 13.32875 | 6 |
| 5 | 1.15406 | 13.34741 | 7 |
| 7 | 1.15414 | 13.35236 | 8 |
| 1 | 1.15425 | 13.36062 | 9 |
| 11 | 1.15425 | 13.36155 | 10 |
| 10 | 1.15433 | 13.36725 | 11 |
| 13 | 1.1544 | 13.37097 | 12 |
| 3 | 1.15449 | 13.37998 | 13 |
| 14 | 1.15476 | 13.39963 | 14 |
| 9 | 1.15483 | 13.40455 | 15 |
| 12 | 1.15527 | 13.43799 | 16 |
| 18 | 1.15546 | 13.4523 | 17 |
| 6 | 1.15553 | 13.45773 | 18 |

Table 4.7: The percentage of decrease of the C_d values with the increase of the weir height

| P=20cm(increase 100%) | | P=15cm(increase 50%) | | P=10cm | D ₅₀ (mm) |
|-----------------------------------|------------|----------------------|------------|------------|----------------------|
| Percentage increase (Cd3-Cd1/Cd1) | Cd3(1,2,3) | Percentage increase | Cd2(1,2,3) | Cd1(1,2,3) | |

Corresponding author: Yakubu, S. K. ✉ Khalees2k1@gmail.com, ✉ Department of Water Resources and Environmental Engineering, A. B. U., Zaria. © 2021 Faculty of Tech. Education, ATBU Bauchi. All rights reserved



| *100% | | (Cd2- Cd1/Cd1) *100% | | | |
|-------|---------|----------------------------|---------|---------|-----------------------|
| -0.12 | 1.15167 | 0.01 | 1.15324 | 1.15310 | Normal |
| 0.01 | 1.15364 | 0.00 | 1.15358 | 1.15353 | |
| -0.10 | 1.15301 | -0.03 | 1.15374 | 1.15412 | |
| -0.12 | 1.15112 | 0.11 | 1.15377 | 1.15249 | |
| -0.21 | 1.15093 | 0.04 | 1.15381 | 1.15339 | |
| 0.08 | 1.15506 | 0.01 | 1.15430 | 1.15419 | |
| -0.08 | 1.15257 | 0.02 | 1.15374 | 1.15347 | |
| | | | | | D ₅₀ =0 |
| -0.02 | 1.15404 | -0.04 | 1.15382 | 1.15426 | |
| 0.91 | 1.15453 | 0.99 | 1.15537 | 1.14408 | |
| -0.01 | 1.15416 | 0.06 | 1.15486 | 1.15422 | |
| -0.18 | 1.15112 | 0.09 | 1.15415 | 1.15316 | |
| -0.51 | 1.14796 | 0.01 | 1.15391 | 1.15382 | |
| 0.02 | 1.15532 | 0.02 | 1.15534 | 1.15514 | |
| 0.04 | 1.15286 | 0.19 | 1.15458 | 1.15245 | |
| | | | | | D ₅₀ =1.18 |
| 0.10 | 1.15583 | -0.02 | 1.15450 | 1.15470 | |
| 0.02 | 1.15509 | 0.08 | 1.15580 | 1.15483 | |
| -0.07 | 1.15376 | 0.06 | 1.15520 | 1.15456 | |
| 0.00 | 1.15303 | 0.12 | 1.15443 | 1.15305 | |
| -0.45 | 1.14895 | 0.02 | 1.15436 | 1.15411 | |
| -0.08 | 1.15540 | -0.08 | 1.15544 | 1.15631 | |
| -0.08 | 1.15368 | 0.03 | 1.15496 | 1.15459 | |
| | | | | | D ₅₀ =4.0 |
| 0.10 | 1.15605 | 0.01 | 1.15501 | 1.15493 | |
| 0.06 | 1.15579 | 0.09 | 1.15612 | 1.15511 | |
| -0.06 | 1.15438 | 0.04 | 1.15550 | 1.15507 | |
| -0.01 | 1.15364 | 0.10 | 1.15496 | 1.15381 | |
| -0.54 | 1.14872 | 0.00 | 1.15491 | 1.15493 | |
| -0.04 | 1.15605 | -0.04 | 1.15599 | 1.15647 | |
| -0.08 | 1.15411 | 0.03 | 1.15542 | 1.15505 | |
| -0.2 | | 0.27 | Average | | |

DISCUSSION OF RESULT

Variation of Cd with (h/P)

The dimensional analysis for the variables affecting Cd value of weirs shows that the value (h/p) (Where h is head of the water on the weir, P height of the weir), has the greatest influence on Cd value. The calculated values of h/P are plotted against the Cd values for each weir and for each surface roughness's as shown in Figure 4. The figure shows that Cd value increase with increasing in h/P values for all the cases. Also, it's evident from these figures that the gradient of the curve fit the points decrease with an increase in weir height, this means that the effect of h/P on Cd values will increase with the increase in weir height.

Finally, the precision of the models in estimating the discharge passing the weir was evaluated using the root-mean-square error (RMSE), mean absolute percentage error (MAE), R^2 (coefficient of determination). The best values of these criteria were 0, 0, and 1 respectively.

$$RMSE = \sqrt{\frac{1}{n} \sum_{j=1}^n (y_j - \hat{y}_j)^2} \quad (12)$$

$$MAE = \frac{1}{n} \sum_{j=1}^n |y_j - \hat{y}_j| \quad (13)$$

$$\hat{R}^2 = 1 - \frac{\sum_{i=1}^n (Y_i - \hat{Y}_i)^2}{\sum_{i=1}^n (Y_i - \bar{Y})^2} = 1 - \frac{\frac{1}{n} \sum_{i=1}^n (Y_i - \hat{Y}_i)^2}{\frac{1}{n} \sum_{i=1}^n (Y_i - \bar{Y})^2} \quad (14)$$

In Eqs. (12)–(14), y is the actual Cd, \hat{y} is their average, n is the number of estimations.

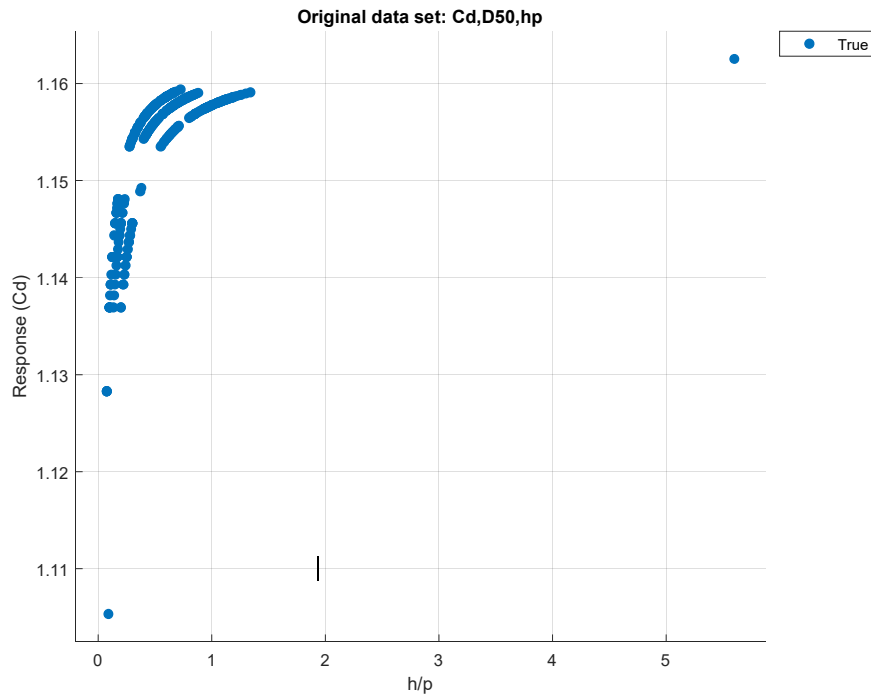


Figure 4: Relation of Cd and h/p using (MLR) model

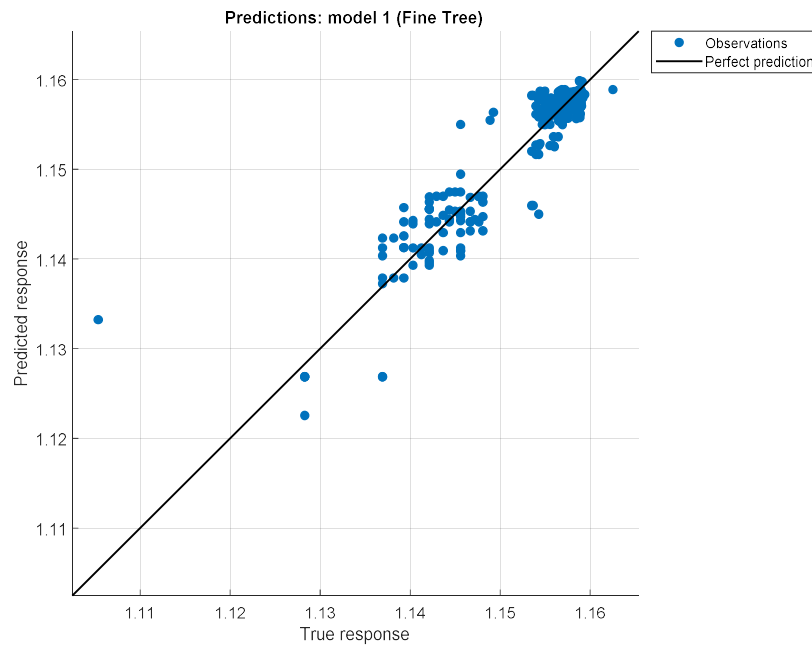


Figure 5: Relation of Cd predicted and Actual value using (MLR) model

Thus, the parameters K_1 , $K_{2,a}$ and b in Equation (10) were determined through regression analysis and Curve Fitting Neural

Network as expressed by Equation (15) as follows:

$$Cd = 0.5785 \left[\frac{D_{50}\theta}{P} \right]^{6.593 \times 10^{-5}} + 0.58 \left[\frac{h}{P} \right]^{0.006761} \quad (15)$$

The model equation has $R^2 = 0.9981$.

Table 7. Sensitivity analysis of Cd's for input parameters with ANN model.

| Function | Training | | Testing | |
|--|------------------------|--------|------------------------|--------|
| | MSE $\times (10^{-4})$ | R^2 | MSE $\times (10^{-4})$ | R^2 |
| $Cd = \left[\frac{D_{50}\theta}{P} \right]$ | 7.5421 | 0.9782 | 7.6801 | 0.9884 |
| $Cd = \left[\frac{h}{P} \right]$ | 3.7313 | 0.9841 | 3.8513 | 0.9971 |
| $Cd = \left(\frac{D_{50}}{P} \theta, \frac{h}{P} \right)$ | 0.1534 | 0.9883 | 0.1635 | 0.9981 |

Table 7, shows the sensitivity analysis of the Coefficient of discharge, Cd. The sensitivity analysis was carried, to evaluate the significance of input variables on the Coefficient of discharge. The sensitivity analysis was performed using the

ANN model due to the high value of the correlation coefficient and minimum error is produced.

Consequently, the parameter $\left(\frac{h}{P} \right)$ was found to be the most effective parameter with $R = 0.9971$, $MSE = 3.8513 \times 10^{-4}$ on the

prediction of C_d . While the function $\left(\frac{D_{50}\theta}{P}\right)$ was found to be the least effective parameter on the prediction of C_d .

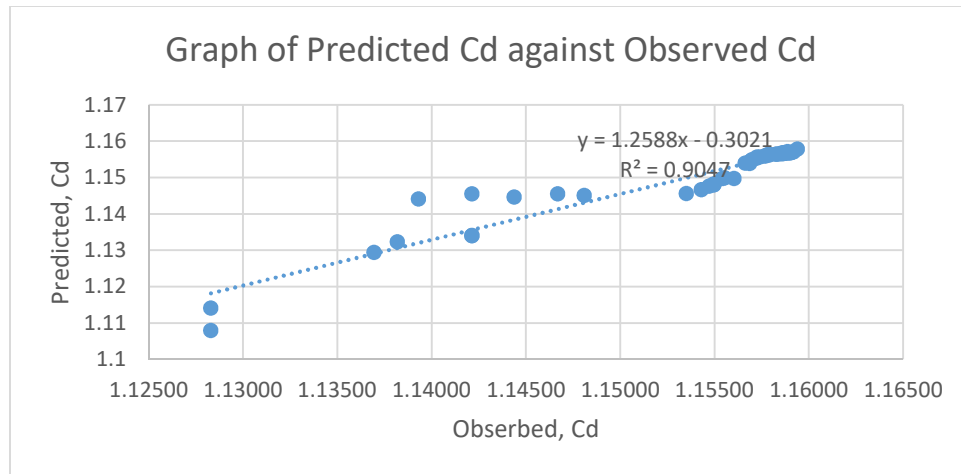


Figure 11: Relation of predicted C_d and observed C_d using (MLP) model

CONCLUSION

By using the equations which have been discussed in the literature, the raw data was calculated and processed using ANN.

Based on the results of the investigation, the following conclusions are reached:

1. C_d increases with the increasing flow rate.
2. The effect of h/P on C_d values increases with the increase in weir height.
3. The effect of the increase of surface roughness on h values will be more on small heights of the crump weir than large ones.
4. C_d decreases from model 1 to model 18 with model 17 having the least C_d close to unity and least percentage error making model 17 to be more efficient.
5. C_d is dependent on the upstream angle, apex angle and downstream angle of the weir. As the upstream angle decreases from 85° to 10° ,

the apex angle increases from 80° to 130° and the downstream angle increases from 15° to 40° the C_d is decreasing.

6. C_d decreases with an increase in the weir height under the same surface roughness. It was found that an increase in weir height from 10 cm to 15cm (50% increase) reduce C_d value by about 0.27%. While an increase in weir height from 10 cm to 20 cm (100% increase) reduce C_d values about - 0.2 %.

RECOMMENDATIONS

The recommendations below are some of the improvements that can be carried out for further study:

1. Depth of weir and width of channel in variable value are suggested to get the best flow rate for hydraulic structure of crump weir design.
2. Calibration device for better data collection suggested using a volume



meter to get the flow rate over a crump weir.

3. Similar study should be carried out using stones and cement models instead of wooden models.

REFERENCES:

- Alauddin, M., Hossain, M., Uddin, M., and Haque, M. (2017). "A Review on Hydraulic and Morphological Characteristics in River Channels Due to Spurs", *World Academy of Science, Engineering and Technology International Journal of Geological and Environmental Engineering*, Vol. 11, No. 4, 397–404.
- Al-Naely, H., Al-Khafaji, Z., & Khassaf, S. (2018). Effect of Opening Holes on the Hydraulic Performance for Crump Weir. *International Journal of Engineering*, 31(12), 2022-2027.
- Al-Sudani, Z. A., Salih, S. Q., & Yaseen, Z. M. (2019). Development of multivariate adaptive regression spline integrated with differential evolution model for streamflow simulation. *Journal of Hydrology*, 573, 1-12.
- Arora, K. R. (2005). *Fluid mechanics and hydraulic machines*. Standard publishers Distributors, 1705-B Nai Sarak, Post Box No.: 1066, Delhi-110006.
- Azimi H, Bonakdari H, Ebtehaj I (2019) Design of radial basis function-based support vector regression in predicting the discharge coefficient of a side weir in a trapezoidal channel. *Appl Water Sci* 9(4):78
- Barr, J., (1910). *Experiments upon the flow of water over triangular notches*. Engineering (London)
- Bengtson Harlan (2010). *Open channel flow measurement*. Bright hub. Retrieved March 6, 2011, from <http://www.brighthub.com/engineering/civil/articles/65701.aspx>
- Bos, M.G. (1989). *Discharge measurement structures*. International Institute for Land Reclamation and Improvement (ILRI), publication 20, Wageningen, The Netherlands.
- Chanson, H. (2004). *The hydraulics of open channel flow: an introduction*. Butterworth-Heinemann, Oxford, UK, 2nd edition. Retrieved March 6, 2011, from <http://www.wikipedia.com>
- Daneshfaraz R, Minaei O, Abraham J, Dadashi S, Ghaderi A (2019) 3-D Numerical simulation of water flow over a broad-crested weir with openings. *ISH J Hydraul Eng*. <https://doi.org/10.1080/09715010.2019.1581098>
- Dolcetti, G., & García Nava, H. (2019). Wavelet spectral analysis of the free surface of turbulent flows. *Journal of Hydraulic Research*, 57(2), 211-226.
- Ghorbani, M. A., & DEGHANI, R. (2017). Comparison of Bayesian neural networks and artificial neural network to estimate suspended sediments in the rivers (case study: Simineh rood).
- Greve, F. V. (1932). *Flow of water through circular, parabolic and triangular vertical notch weirs*. Purdue Univ. Eng. Bull., 16, No. 2, Res. Series 40
- Haghiabi, A. H., Parsaie, A., & Ememgholizadeh, S. (2018). Prediction of discharge coefficient of triangular labyrinth weirs using Adaptive Neuro Fuzzy Inference System. *Alexandria Engineering Journal*, 57(3), 1773-1782.
- Heidari, E., Sobati, M. A., & Movahedirad, S. (2016). Accurate prediction of nanofluid viscosity using a multilayer perceptron artificial neural network (MLP-ANN).



- Chemometrics and intelligent laboratory systems*, 155, 73-85.
- Herschly R. W. (1978), *Hydrometry principles and practices*. Department of the Environment Water Data Unit; Reading, A Wiley – Interscience Publication, John Wiley and Sons
- Hertzler, R. A. (1938). *Determination of a formular for the 120° V-notch weir*. Civil Engineering, 756.
- Jan Chyan-Deng, Chia-Jung Chang, and Feng-Hao Kuo (2009), Experiments on Discharge Equations of Compound Broad-Crested Weirs. *Journal of Irrigation and Drainage Engineering © Asce / July/August 2009 / 511*
- Jan Chyan-Deng, Chia-Jung Chang, and Ming-His Lee (2006), Discussion of Design and calibration of compound sharp-crested weir by J. Martinez et al. *Journal of Hydraulic Engineering*, 132(8), 868–871.
- Karami, H., Karimi, S., Bonakdari, H., & Shamsirband, S. (2018). Predicting discharge coefficient of triangular labyrinth weir using extreme learning machine, artificial neural network and genetic programming. *Neural Computing and Applications*, 29(11), 983-989.
- King, H. W. (1916). *Flow of water over right-angled V-notch weir*. Univ. Mich. Technic. 29, No. 3, 189
- Khalifa, S. Y., & Umar, A. (2018). Evaluation of Unsteady Open Channel Flow Characteristics over Crump Weir. *ATBU Journal of Science, Technology and Education*, 6(4), 306-315.
- Lenz, A. T., (1943). *Viscosity and surface tension effects in V-notch weir coefficients*. Trans. A.S.C.E., 108
- Martinez J., Reza J., Morillas M. T., and López J. G.; (2005), Discussion of Design and Calibration of a Compound Sharp-Crested Weir. *Journal of Hydraulic Engineering © ASCE Vol. 131, No.2, pp. 112-116*.
- Mehr, A. D., Nourani, V., Kahya, E., Hrnjica, B., Sattar, A. M., & Yaseen, Z. M. (2018). Genetic programming in water resources engineering: A state-of-the-art review. *Journal of Hydrology*, 566, 643-667.
- Moazamnia M, Hassanzadeh Y, Nadiri AA, Khatibi R, Sadeghfam S (2019) Formulating a strategy to combine artificial intelligence models using Bayesian model averaging to study a distressed aquifer with sparse data availability. *J Hydrol* 571:765–781
- Muhammad, M. M., Yusof, K. W., Mustafa, M. R. U., Zakaria, N. A., & Ab Ghani, A. (2018). Prediction models for flow resistance in flexible vegetated channels. *International journal of river basin management*, 16(4), 427-437.
- Nadiri AA, Sedghi Z, Khatibi R, Sadeghfam S (2018) Mapping specific vulnerability of multiple confined and unconfined aquifers by using artificial intelligence to learn from multiple DRASTIC frameworks. *J Environ Manage* 227:415–428
- Piratheepan M., Winston N.E.F., and Pathirana K.P.P. (2006), Discharge measurements in open channels using compound sharp-crested weirs. *Journal of the Institution of Engineers, Sri Lanka Vol. xxx, No. 03, pp.31-38*.
- Richard H. French (1985), "Open-Channel Hydraulics." Mc Graw Hill, New York.
- Rickard C., Day R., Purse glove J., 2003, "River Weirs – Good Practice Guide", Environment Agency, Rio House, Waterside Drive, Aztec West, Almondsbury, Bristol, BS32 4UD,.



- Roushangar K, Alami MT, Majedi Shiri J, Asl M (2017) Determining discharge coefficient of the labyrinth and arced labyrinth weirs using support vector machine. *Hydrol Res* 49(3):924–938
- Sadeghfam S, Daneshfaraz R, Khatibi R, Minaei O (2019) Experimental studies on scour of Supercritical flow jets in upstream of screens and modelling scouring dimensions using artificial intelligence to combine multiple models (AIMM). *J Hydro inform.* <https://doi.org/10.2166/hydro.2019.076>
- Sanikhani, H., Kisi, O., Maroufpoor, E., & Yaseen, Z. M. (2019). Temperature-based modeling of reference evapotranspiration using several artificial intelligence models: application of different modeling scenarios. *Theoretical and applied climatology*, 135(1-2), 449-462.
- Sattar, A. A., Elhakeem, M., Rezaie-Balf, M., Gharabaghi, B., & Bonakdari, H. (2019). Artificial intelligence models for prediction of the aeration efficiency of the stepped weir. *Flow Measurement and Instrumentation*, 65, 78-89.
- Shen, J. (1960). *Discharge characteristics of triangular-notch thin-plate weirs*. U.S. Dept. of Interior, Geological Survey, draft for I.S.O.
- Simon A. L. (1976). *Practical hydraulics*. John Wiley and Sons, Inc. New York. London. Sydney. Toronto.
- Yousif, A. A., Sulaiman, S. O., Diop, L., Ehteram, M., Shahid, S., Al-Ansari, N., & Yaseen, Z. M. (2019). Open channel sluice gate scouring parameters prediction: different scenarios of dimensional and non-dimensional input parameters. *Water*, 11(2), 353.
- Zahabi H, Torabi M, Alamatian E, Bahiraei M, Goodarzi M (2018) Effects of geometry and hydraulic characteristics of shallow reservoirs on sediment entrapment. *Water* 10(12):1725
- Zhou Q, Zhou H, Zhou Q, Yang F, Luo L, Li T (2015) Structural damage detection based on posterior probability support vector machine and Dempster-Shafer evidence theory. *Appl Soft Comput* 36:368–374
- Zounemat-Kermani, M., & Mahdavi-Meymand, A. (2019). Hybrid meta-heuristics artificial intelligence models in simulating discharge passing the piano key weirs. *Journal of Hydrology*, 569, 12-21.